

Random Neighbor Theory of the Olami-Feder-Christensen Earthquake Model

Hans-Martin Bröker¹ and Peter Grassberger^{1,2}

¹ Physics Department, University of Wuppertal, D-42097 Wuppertal, Germany

² HLRZ c/o Forschungszentrum Jülich, D-52425 Jülich, Germany

May 11, 2019

Abstract

We derive the exact equations of motion for the random neighbor version of the Olami-Feder-Christensen earthquake model in the infinite-size limit. We solve them numerically, and compare with simulations of the model for large numbers of sites. We find perfect agreement. But we do not find any scaling or phase transitions, except in the conservative limit. This is in contradiction to claims by Lise & Jensen (Phys. Rev. Lett. **76**, 2326 (1996)) based on approximate solutions of the same model. It indicates again that scaling in the Olami-Feder-Christensen model is only due to partial synchronization driven by spatial inhomogeneities. Finally, we point out that our method can be used also for other SOC models, and treat in detail the random neighbor version of the Feder-Feder model.

1 Introduction

During the last ten years more than 2000 publications were concerned with the idea of self-organized criticality (SOC) proposed by Bak, Tang and Wiesenfeld (BTW) [1]. They introduced a non-equilibrium system, the so-called sandpile model, which is driven slowly by adding single sand grains at random positions. Without any control parameter to fine-tune, it evolves into a critical state. In this state the system reacts to the external drive with a series of relaxation events (avalanches). It becomes critical in the sense that the spatial and temporal distributions of these avalanches obey power laws, indicating that any characteristic scales in space and time are lost. The attribute ‘self-organized’ is to stress the absence of a fine-tuned control parameter.

A crucial point in understanding the robust scaling of the BTW model is the existence of a conservation law [5]: the total amount of sand in the system is conserved, if boundary effects and external perturbations are neglected.

In the frame of this concept, Olami, Feder, and Christensen (OFC) introduced a nonconservative ‘continuous cellular automaton’ [2] as a specific realization of the two-dimensional Burridge–Knopoff earthquake model [4]. Details of this model will be described below. In contrast to the BTW model it is not conservative in general. It involves a parameter α , and a conservation law holds only for a specific value $\alpha = \alpha_c$. It was found in [2, 3] and subsequent simulations [6] that the system displays power law behavior in a wide range of the control parameter α (not only near α_c), and the critical exponents depend on α . Thus the model seems to show SOC, and conservation seems not a necessary condition.

But, on the other hand, it seems that spatial inhomogeneities are crucial for the observation of scaling in the OFC model [6, 7, 8]. In the original paper by OFC the boundary conditions (bc) were not periodic, which induced an inhomogeneity with a diverging length scale in the thermodynamic limit. This inhomogeneity of the bc leads to partial synchronization in the bulk which is both driven and destroyed by the boundary [6]. Subsequent simulations with periodic bc showed no scaling [9, 6], as did also simulations with frozen randomness but without diverging length scales [10, 11]. The basic source of scaling in the OFC model is the slow build-up of large coherent domains in which the system itself is homogeneous, but which are driven by regions where the system is not homogeneous.

Although the definitions of these SOC models are simple, and they are easily simulated on a computer, only few exact results are known. Most of the difficulties in the analytical treatment arise from the spatial correlations due to the interactions of the particles. In a mean-field theory, which is the first step towards a detailed understanding, these correlations are simply neglected. A more refined strategy to avoid spatial correlations is to replace the nearest neighbors interactions by interactions between random sites. For the OFC model this was already attempted by [12]. But in that paper additional assumptions and approximations were made which are hard to justify. With these assumptions, a transition was found from non-SOC to SOC at α significantly less than α_c . This is very surprising, as we argued above that spatial structures are crucial for the emergence of scaling, and any such structures are of course

eliminated in the random neighbor version.

In the following we study the random neighbor model in detail without any further approximations. We will be led to a complete set of equations which allow us to calculate numerically all the relevant quantities. We will see that there is no SOC in the dissipative regime of the control-parameter. In the case of conservation the exact solution shows that the system becomes a critical branching process equivalent to critical percolation on a Bethe tree, and the critical exponents take their mean-field values.

2 The model

The model lives on a set of N sites, each of them equipped with a continuous stress (or ‘force’) variable z_i . Each z_i can take any value ≥ 0 , but only values < 1 are stable. After having initialized each site with a randomly chosen value $z_i \in [0, 1[$, the system evolves according to the following rules:

(i) All z_i are simultaneously and continuously increased with the same speed $v = 1$.

(ii) If any z_i exceeds the threshold value 1 the above driving stops, and the forces are redistributed in the following way:

All unstable sites discharge simultaneously,

$$z_i \rightarrow 0 \quad \forall z_i \geq 1. \quad (1)$$

For each of these discharging sites n random “neighbors”, j_1, \dots, j_n , are chosen and their stress variables are increased by a fixed fraction of z_i .

$$z_{j_k} \rightarrow z_{j_k} + \alpha z_i \quad k = 1, \dots, n \quad (2)$$

The integer n is constant but otherwise arbitrary. If the application of eq. (2) creates new unstable sites, rule (ii) is again applied in the next time step, again simultaneously for all unstable sites. This procedure is repeated until all sites are stable. After that, the system is again driven according to rule (i), until at least one site with $z_i = 1$ appears. A series of causally connected discharging events is called an earthquake or an avalanche. Its size s is measured by the total number of discharges. If a site discharges m times during an avalanche, it is counted m -fold in the calculation of s . The duration t of an earthquake is defined as the number of sweeps through the lattice necessary to get a stable configuration. Obviously s as well as t is always ≥ 1 .

The parameter α which controls the dissipation can take any value between 0 and $1/n$ ($\alpha > 1/n$ is unphysical since sooner or later an infinite and ever growing avalanche would occur). Only for $\alpha = 1/n$ the system is conservative. Note that the randomness of the neighbors appearing in eq. (2) is annealed: For each discharging event, the n random neighbors are chosen anew. Obviously this prevents that any spatial correlations in the values of z to build up.

The numerical calculations as well as the simulations are restricted to the case $n = 4$. Obviously this is most appropriate for a mean-field theory of the two-dimensional OFC-model. But our analytic results are more general and hold for any $n \geq 2$.

As well known, the original (nearest neighbor) version of the model is very sensitive to the choice of bc's [9, 6]. Any bc other than periodic introduce inhomogeneities which are crucial in building up the spatial structures which manifest themselves in non-trivial avalanches [6, 7, 8]. For the random neighbor version, non-periodic bc were used in [12]. This also introduces spatial inhomogeneity which is however completely irrelevant for the dynamics, 'space' being a dummy concept in a random neighbor model. In addition, the bc used in [12] lead to specific finite size corrections which might be not easy to disentangle from the true asymptotic behavior. In contrast, we treat all sites equally in the present paper, mimicking thereby periodic bc. In addition, we shall only study the infinite size limit. More precisely, we shall formally work with a finite number N of sites, but will understand that we are only interested in the limit $N \rightarrow \infty$. For finite sizes there are correlations which make the study of the model rather awkward.

3 Random Neighbor Theory

In the OFC model, there is a finite chance that two sites become unstable simultaneously during the continuous increase (i). It arises from the non-zero probability that two sites which had discharged in the same previous earth quake have not been hit by a discharging neighbor (or have been hit by the same neighbors) until they reach $z = 1$. In the lattice version this implies that the notion of an earth quake itself becomes a bit delicate: should we consider an event which was triggered simultaneously by two sites as one earth quake or two? In the off-lattice version we still have a non-zero chance for such events. But on an infinite lattice the sub-quakes following each unstable site will not overlap. Thus they will evolve completely independently. This means that the model becomes effectively abelian [13] in the sense that we can change the order of updates in different sub-events. Also, we can associate earth quakes uniquely with the original unstable sites which triggered them. In the following, we will always define earth quakes in this way. An event which started with k sites becoming unstable is counted as k earth quakes, separated by infinitesimal time delays and taking place in arbitrary order.

So we can assume without loss of generality that after the relaxation of an earthquake there is exactly one site which has a stress value greater than all the others, and which will be the seed of the next avalanche. The value of this stress immediately after the earthquake has stopped will be called z_m . Its mean value, averaged over all earthquakes, is denoted by $\overline{z_m}$. Since we consider the large system limit, z_m will not be correlated with the size of the previous avalanche. This is our crucial assumption, and it depends on the fact that we can neglect 'global' avalanches whose size is comparable to the total size of the system. In this limit the model thus becomes a branching process with time dependent branching rates. We shall later verify that this assumption is self consistent, and is true in simulations.

The average increase of the force on each of the N sites between two earth quakes due to the external driving is then given by $1 - \overline{z_m}$. On the other hand, each discharge dissipates an average value of $(1 - n\alpha)\overline{z_{unst}}$, where $\overline{z_{unst}}$ is the mean force on the unstable

sites, averaged over all discharging events. In the stationary state, when $\sum z_i$ fluctuates around a constant value, the external increase must be exactly compensated by the average dissipation. This gives an exact formula involving the average earthquake size $\langle s \rangle$ defined as the mean number of discharges per earth quake,

$$(1 - n\alpha) \overline{z_{\text{unst}}} \langle s \rangle = N(1 - \overline{z_m}) . \quad (3)$$

Notice that the product of averages on the l.h.s. does not result from a factorization approximation but from the definition of $\overline{z_{\text{unst}}}$, and is exact. Therefore, this equation is correct even if the above mentioned simplifying assumptions are not true, and holds thus also in the fixed neighbor version of the model. Since the left hand side of this equation remains finite for $N \rightarrow \infty$ (as long as $\alpha < 1/n$), we see that $1 - \overline{z_m} \propto 1/N$.

On the other hand, since the force increase between earth quakes is assumed to be with velocity $v = 1$, the average time between two earth quakes is given by $1 - \overline{z_m}$. On a ‘macroscopic’ time scale where we neglect the duration of earth quakes compared to the inter-quake times (this assumption is inherent in the model), the *toppling rate* is thus given by

$$\sigma = \frac{\langle s \rangle}{N(1 - \overline{z_m})} = \frac{1}{(1 - n\alpha)\overline{z_{\text{unst}}}} . \quad (4)$$

This tells us how frequently each site discharges per time unit. The rate to *be hit* according to eq.(2) is then given by $n\sigma$.

Let $P(z)$ be the probability density for a given site to have a force value z (from now on, we shall consider only $N = \infty$). Obviously, $P(1)$ is the rate with which new earth quakes are initiated, while $P(0) = \sigma$ is the rate with which new force-free sites are created by discharges. Therefore,

$$\langle s \rangle = P(0)/P(1) . \quad (5)$$

Similarly, $P_j(z)$ denotes the joint probability density that a site has a value z and was hit exactly j -times since its last discharge. Since we consider only $N = \infty$ and have argued that global avalanches are negligible in this limit, $P(z)$ and $P_j(z)$ do not fluctuate with time. Obviously, we have

$$P(z) = \sum_{j=0}^m P_j(z) \quad z \in [0, 1] . \quad (6)$$

Because a hit increases z at least by an amount α , each $P_j(z)$ vanishes exactly for $z < j\alpha$. Therefore the upper limit m in the above sum is given by the largest integer for which $m\alpha \leq 1$. For later use we define the integrated distribution as

$$\mathcal{P}(z) = \int_z^1 P(z') dz' . \quad (7)$$

To obtain $P_0(z)$ we notice that the probability to be hit exactly k times during a time interval z , when the rate is $n\sigma$, is given by the Poisson distribution

$$\pi_k(z) = \frac{1}{k!} (n\sigma z)^k e^{-n\sigma z} . \quad (8)$$

This leads to

$$P_0(z) = \sigma \pi_0(z) = \sigma e^{-n\sigma z}. \quad (9)$$

The other $P_j(z)$ depend on the distribution of the amount Δz which a site receives when it gets hit by a discharge. This in turn depends on the distribution of forces of unstable sites at the moment of their discharge. We denote the density of this distribution by $C(z)$. It is related to $\overline{z_{\text{unst}}}$ by

$$\overline{z_{\text{unst}}} = \int_1^\infty z C(z) dz. \quad (10)$$

(Here and in the following, integrals over functions with δ -peaks at the integration limits are understood as containing all contributions from these peaks, $\int_a^b f(x) dx \equiv \lim_{\epsilon \rightarrow 0} \int_{a-\epsilon}^{b+\epsilon} f(x) dx$.) The first site of any earthquake discharges exactly with $z = 1$. This gives a delta contribution to $C(z)$, with relative weight $1/\langle s \rangle$. We can therefore make the ansatz

$$C(z) = \frac{1}{\langle s \rangle} \delta(z - 1) + \tilde{C}(z). \quad (11)$$

The second term corresponds to all subsequent discharges. About the function $\tilde{C}(z)$ we know that it has to vanish for all z outside the interval $[1, 1/(1 - \alpha)]$. The upper limit would be reached if an infinite earthquake contained a series of successive hits onto sites with maximum value $z = 1$. This upper limit could be surpassed only if a site were hit simultaneously by two discharges, but the chance for this is zero on an infinite lattice. The amount of force Δz that a discharging site drops onto each of the n random neighbors is then distributed according to

$$Q_1(\Delta z) = \alpha^{-1} C(\Delta z / \alpha), \quad \text{supp } Q_1 = [\alpha, \alpha / (1 - \alpha)]. \quad (12)$$

Similar to eq. (11) we can write $Q_1(\Delta z)$ as

$$Q_1(\Delta z) = \frac{1}{\langle s \rangle} \delta(\Delta z - \alpha) + \tilde{Q}_1(\Delta z). \quad (13)$$

The convolution integrals

$$Q_k(\Delta z) = \int_\alpha^{\Delta z} Q_{k-1}(\Delta z - \Delta z') Q_1(\Delta z') d\Delta z', \quad k \geq 2 \quad (14)$$

then give us the probability densities for the total increase of force when a site was hit exactly k times. Note that $Q_k(\Delta z)$ vanishes for Δz outside the interval $[k\alpha, k\alpha / (1 - \alpha)]$. We see finally that every $P_j(z)$ has to obey

$$\begin{aligned} P_j(z) &= P_0(0) \int_{j\alpha}^z \pi_j(z - \Delta z) Q_j(\Delta z) d\Delta z \\ &= \frac{\sigma}{j!} \int_{j\alpha}^z (n\sigma(z - \Delta z))^j e^{-n\sigma(z - \Delta z)} Q_j(\Delta z) d\Delta z. \end{aligned} \quad (15)$$

Let us now come back to the function $\tilde{C}(z)$ which describes the distribution of sites which have become unstable by being hit by a discharge. It is obtained by the

convolution of the distribution of (stable) sites before they are hit, with the distribution of amounts received during the destabilizing discharge,

$$\tilde{C}(z) = n \Theta(z - 1) \int_{\alpha}^{\alpha/(1-\alpha)} P(z - \Delta z) Q_1(\Delta z) d\Delta z \quad (16)$$

Here $\Theta(x)$ is the Heaviside step function. It takes into account that $\tilde{C}(z)$ is supposed to describe only those sites which actually do become unstable. The factor n takes into account that each discharge event — the probability density of which is given by the integrand — gives rise to n potentially unstable sites. The integration limits are given by the support of Q_1 , see eq.(12).

Let us now consider the integral of $\tilde{C}(z)$ over all z . Interchanging the integrations we obtain

$$\int_1^{\infty} \tilde{C}(z) dz = n \int_{\alpha}^{\alpha/(1-\alpha)} d\Delta z Q_1(\Delta z) \int_1^{\infty} P(z - \Delta z) dz . \quad (17)$$

The inner integral on the rhs. is just $\mathcal{P}(1 - \Delta z)$ (see eq.(7)), while the left hand side is equal to $1 - 1/\langle s \rangle$ due to eq.(11). Rearranging terms we arrive thus at a second equation for $\langle s \rangle$,

$$\langle s \rangle = \left[1 - n \int_{\alpha}^{\alpha/(1-\alpha)} \mathcal{P}(1 - z) Q_1(z) dz \right]^{-1} . \quad (18)$$

We claim that the above equations are complete in the sense that they fix the solution uniquely, for each $\alpha < 1/n$. To show this, and to provide also a practical method to solve them numerically for not too large α , we give a recursion scheme which converges to the solution as the iteration level r tends to infinity, at least for sufficiently small α . For larger values of α the recursion might not be practical, but the set of equations should still fix the solution by continuity. Notice that different recursion schemes are in principle possible where the order of replacements is changed in various places.

To start the recursion, we select a desired accuracy η and choose the initial distribution $Q_1(z)^{(0)}$ in some arbitrary way. It need not even be normalized. For small α , a good choice is $Q_1(z)^{(0)}$ constant. For $\alpha \approx 1/n$ we can also take $Q_1(z)^{(0)} = \delta(z - 1/n)$. In the recursive step from $r - 1$ to r we do the following:

- (1) (re-)normalize $Q_1(z) = \text{const} \times Q_1^{(r-1)}(z)$ with $\text{const} = [\int Q_1^{(r-1)}(z) dz]^{-1}$;
- (2) compute σ from eqs.(4), (10), and (12),

$$\sigma = \alpha \left[(1 - n\alpha) \int_{\alpha}^{\alpha/(1-\alpha)} Q_1(z) z dz \right]^{-1} ; \quad (19)$$

- (3) compute $Q_k(z)$ for $k > 1$ by means of eq.(14);
- (4) compute $P_0(z) = \sigma e^{-n\sigma z}$, compute $P_k(z)$ for $k > 0$ by means of eq.(15), and obtain $P(z)$ as $\sum_k P_k(z)$;
- (5) compute the new $\langle s \rangle$ from eq.(5);
- (6) compute the new $Q_1(z)$ from eqs.(12), (11), and (16),

$$Q_1^{(r)}(z) = \frac{1}{\langle s \rangle} \delta(z - \alpha) + \frac{n}{\alpha} \Theta(z - \alpha) \int_{\alpha}^{\alpha/(1-\alpha)} P(z/\alpha - \zeta) Q_1(\zeta) d\zeta ; \quad (20)$$

- (7) if σ or $\langle s \rangle$ have changed by a fraction larger than η , then goto (1);
- (8) verify that the normalization constant in step (1) is unity within some acceptable error, and that $\langle s \rangle$ satisfies eq.(18).

We have not shown formally that this iteration converges always, but we have done extensive numerical investigations. The scheme converges very fast and stably for small α , but convergence is slowed down when $\alpha \rightarrow 1/n$. For this reason we had problems to obtain solutions for $\alpha \geq 0.24$, although the recursions shows no sign for divergence even in such extreme cases. Also, numerical errors in the integration routines tend to accumulate for $\alpha \rightarrow 1/n$, rendering in particular the estimate of $\langle s \rangle$ problematic. Since the integrands are not analytic functions, it does not make sense to use very sophisticated integration routines. We used the extended trapezoidal rule with up to 10^4 points.

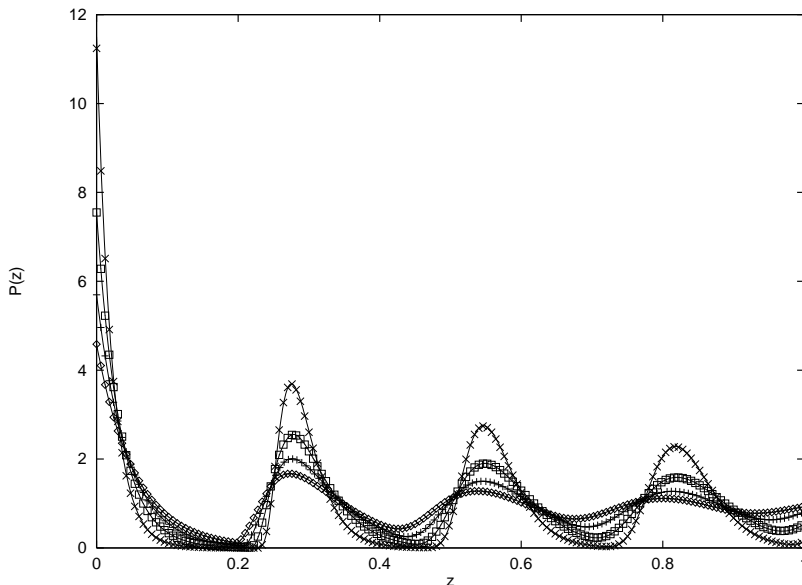


Figure 1: Probability density $P(z)$ against z . The continuous lines are the predictions from the theory and the points show the results obtained from simulations. They fall perfectly on top of each other on the scale of this figure. The four curves are for $\alpha = 0.20, 0.21, 0.22,$ and 0.23 , in order of increasing sharpness of the peaks.

Results for $n = 4$ are shown in fig. 1, where we also compare with straightforward simulations of eqs.(1),(2). For the latter we typically used $N = 10^6$ to 8×10^6 , and discarded transients of up to 2×10^6 iterations. No difference between theory and simulation is detectable in fig. 1. This shows that the numerical integration was sufficiently accurate, the iterations had converged, N was sufficiently large to have negligible finite size corrections, and the discarded transients were sufficiently long. Qualitatively, fig. 1 is similar to fig.1 in [12], but the first peak in that paper seems much too high. It is not clear whether this results from the bc used in that paper or from transients. For $\alpha = 0.23$, we find $P(0) \approx 11.5$ both from simulations and from the analytic solution, while $P(0) \approx 33$ is quoted in [12].

In fig. 2 we show σ and $\langle s \rangle$ as functions of $\epsilon = 1 - 4\alpha$. We see that $\sigma \approx 1/\epsilon$,

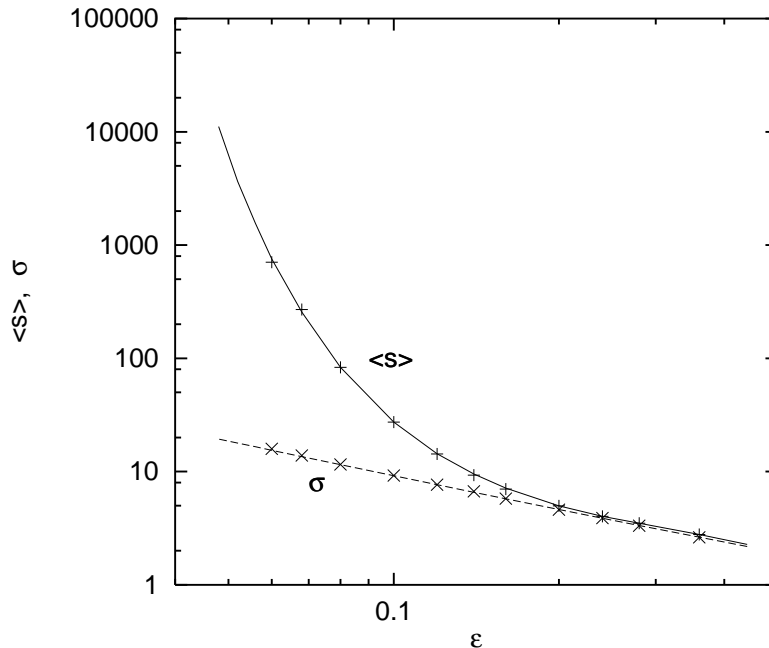


Figure 2: Log-log plot of σ and $\langle s \rangle$ against $\epsilon = 1 - 4\alpha$. Continuous lines are from theory, points from simulations.

while $\langle s \rangle$ diverges much faster when $\alpha \rightarrow 1/4$. Finally, in fig. 3 we show $\tilde{Q}_1(z)$. This shows a very interesting qualitative change as α approaches $1/4$. For $\alpha < 0.23$, $\tilde{Q}_1(z)$ is centered at $z < 1/4$. Its center moves to the right as α increases, reaching a value slightly larger than $1/4$ for $\alpha \approx 0.233$. After that, its center moves very little, and it just shrinks slowly to a δ -function centered at $1/4$.

The most important result is that we see no hint of any singularity for $\alpha < 1/4$, as predicted in [12], and we also see no mechanism which could lead to such a singularity. Indeed, we can prove rigorously that $\langle s \rangle < \infty$ for all $\alpha < 1/n$. This follows simply from the fact that $\sigma \leq 1/(1 - n\alpha)$ due to eq.(4), and $\langle s \rangle = \sigma/P(1) \leq \sigma/P_0(1) = e^{n\sigma}$ due to eqs.(5) and (9). Conversely, this argument shows that $P(1)$ must tend to 0 for $\epsilon \rightarrow 0$, as also shown by the numerics.

According to [12], a singularity with $\langle s \rangle \rightarrow \infty$ should occur for $n = 4$ at $\alpha = 2/9 = 0.222\dots$. We believe that this is due to unjustified assumptions made in [12]. Another important result is that $P(z)$ is finite and non-zero at $z = 1$ and at $z = 0$. This shows that ‘global’ earth quakes have indeed no effect, as they would lead to a depletion at $P(z)$ at $z = 1$ or an infinity at $z = 0$ due to eq.(5).

4 The Limit $\alpha \rightarrow 1/n$

Figure 1 suggests that $P(z)$ tends to a sum of four delta peaks at multiples of α , for $\alpha \rightarrow 1/4$. More generally, we expect $P(z)$ to tend towards a sum of n delta peaks at $z = k/n$, $k = 0, \dots, n - 1$ (this is reminiscent of a generalized sandpile model with

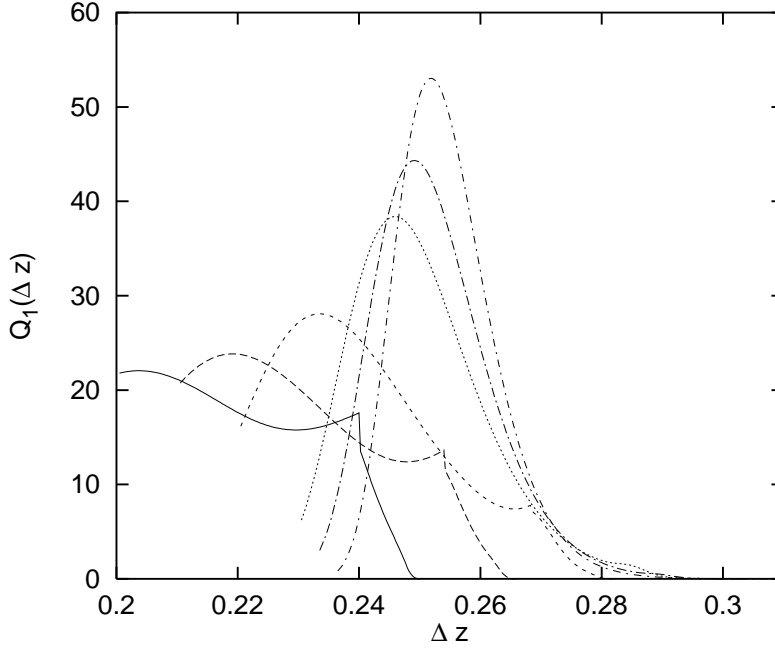


Figure 3: $\tilde{Q}_1(\Delta z)$ against Δz , for the same values of α as in fig. 1, and in addition for $\alpha = 0.233$ and $\alpha = 0.236$. For clarity only theoretical predictions are shown. The cusps are at $\Delta z = \alpha + \alpha^2$ and correspond to the maximal Δz transferred by first generation descendents of the avalanche seed.

real-valued heights by Zhang [14]). We shall see that this is indeed a valid solution after proper rescalings of σ and $\langle s \rangle$.

Formally we introduce

$$\epsilon = 1 - \alpha n, \quad (21)$$

and consider the limit $\epsilon \rightarrow 0$. We shall argue that a self consistent solution for $P(z)$ in this limit is a sum of delta peaks. If this is true, only sites which have already $z \approx (n-1)/n$ will become unstable by receiving an extra $\Delta z \approx 1/n$, and hence $z_{\text{unst}} \rightarrow 1$ for $\epsilon \rightarrow 0$. From this we see on the one hand that $\sigma = 1/\epsilon$ to leading order in $1/\epsilon$, which in turn gives $\sigma \pi_k(z) \rightarrow n^{-1} \delta(z)$ for each value of k . On the other hand it gives $C(z) = \delta(z-1)$ and $Q_1(\Delta z) = \delta(\Delta z - 1/n)$. The latter implies $Q_k(\Delta z) = \delta(\Delta z - k/n)$ for any $k \geq 2$, which finally gives

$$P(z) = \frac{1}{n} \sum_{j=0}^{n-1} \delta(z - j/n), \quad (22)$$

i.e. our initial assumption was self consistent.

In spite of the simplicity of this solution, we should be careful in interpreting it, as several limits are involved. The easiest way is to take first the infinite volume limit, and then $\epsilon \rightarrow 0$. If we want to take the limit $\epsilon \rightarrow 0$ first, we have to use absorbing sites which mimic absorbing bc's, but it is not a priori clear how their number should scale

with N (for a related problem in a mean field version of the abelian sandpile model, see [15, 16]).

While the behavior exactly at $\alpha = 1/n$ is thus well understood, we were not able to find an analytic solution for finite ϵ . But we can give approximate solutions for small ϵ , and predict the behavior of $\langle s \rangle$ for $\epsilon \rightarrow 0$. For small but finite ϵ , we approximate each $Q_j(z)$ by a delta function at $z = j/n$. Then $P_j(z)$ is roughly given by

$$P_j(z) \approx \Theta(z - j/n) \frac{\sigma}{j!} [(z - j/n)\sigma]^j e^{-(z-j/n)\sigma}. \quad (23)$$

From this, eq.(5), and the fact that $P(0) = \sigma$, we get

$$\langle s \rangle = \sigma/P(1) \approx \sigma/P_{n-1}(1) \approx \frac{(n-1)!}{\sigma^{n-1}} e^\sigma \approx (n-1)! \epsilon^{n-1} e^{1/\epsilon}. \quad (24)$$

There are substantial corrections to this, mainly from the contribution of $P_n(1)$ to $P(1)$, which are hard to estimate. Thus, the actual values of $\langle s \rangle$ are smaller than given by eq.(24), but eq.(24) gives the correct trend. In particular, it explains why $\langle s \rangle$ diverges extremely fast for $\alpha \rightarrow 1/n$, making simulations in this limit very difficult.

5 Earth Quake Statistics

In the previous sections we have only studied the force distribution and the average earth quake size. In order to discuss the distribution of earth quake sizes and durations, we need some more definitions and some basic results from the theory of branching processes as found e.g. in [17].

For any integer $i \geq 1$ we define p_i as the probability that a site becomes unstable if it is hit by a discharge event during the $(i-1)$ -st generation of an earth quake, and will therefore discharge itself in the i -th generation. For the first generation, p_1 is the probability that a site which receives $\Delta z = \alpha$ gets unstable. Thus, simply $p_1 = \mathcal{P}(1 - \alpha)$. For general α , the other probabilities p_i depend on the height distribution of the unstable sites in the previous generation. But for $\epsilon \rightarrow 0$ all discharging sites have $z = 1$, and p_i is simply the probability that the hit site is in the $(n-1)$ -st peak, $p_i = p = 1/n$ for all $i > 0$.

In the following we shall therefore discuss only the case $\epsilon = 0$, deferring the general case to the end of this section.

We assume thus that $p_i = p = 1/n$ for all $i > 0$. The probability that an unstable site creates l unstable offsprings in the next generation is then given by

$$w_l = \binom{n}{l} (1-p)^{n-l} p^l \quad (25)$$

with the generating function

$$g(u) = \sum_{l=0}^n u^l w_l = (1-p + up)^n. \quad (26)$$

With the use of $g(u)$ it becomes very easy to calculate recursively the distributions of the size and the duration of the earthquakes. In order to do this we introduce the iterates

$$\begin{aligned} g_0(u) &= u, & g_1(u) &= g(u), \\ g_{m+1}(u) &= g[g_m(u)], & m &= 1, 2, \dots, \end{aligned} \quad (27)$$

The probability that the earthquake stops in the t -th time step is given by [17]

$$\mathcal{P}_t = g_t(0) - g_{t-1}(0) \quad \text{with} \quad t = 1, 2, \dots \quad (28)$$

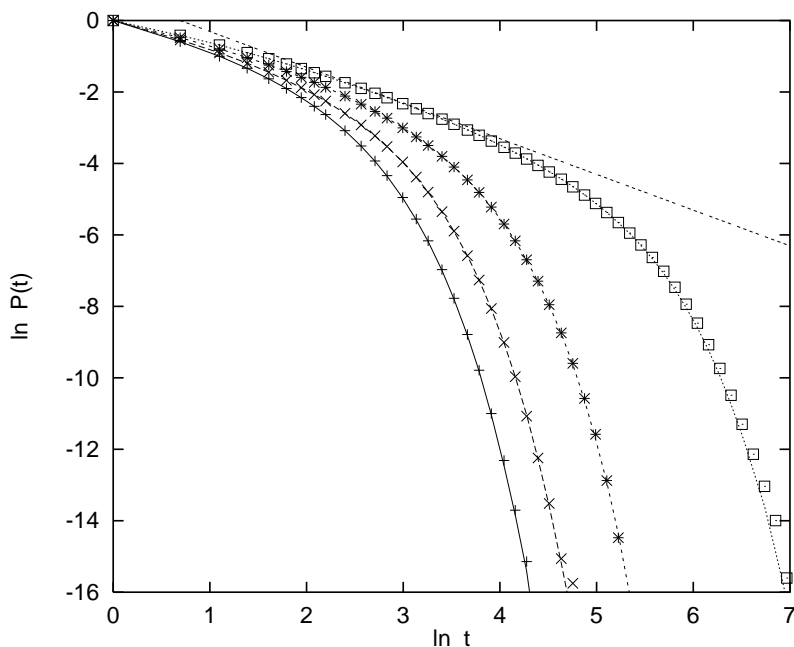


Figure 4: The integrated distribution P_t . Again, lines show the theoretical predictions and points are from simulations. Increasing from left to right, α takes the same values as in fig. 1. The dashed line shows eq. (32).

The integrated distribution

$$P_t = \sum_{t'=t}^{\infty} \mathcal{P}_{t'} = 1 - g_{t-1}(0) \quad (29)$$

denotes the probability that an avalanche lasts for $\geq t$ time steps. Eq. (29) can be used directly to calculate P_t for small t , whereas for large t we use the asymptotic behavior. The chain of identities

$$\begin{aligned} P_{t+1} &= 1 - g_t(0) \\ &= 1 - g(g_{t-1}(0)) \\ &= 1 - g(1 - P_t) \\ &= 1 - (1 - pP_t)^n \end{aligned} \quad (30)$$

leads to

$$\frac{d}{dt}P_t \simeq P_{t+1} - P_t = -\binom{n}{2}p^2P_t^2 + o(P_t^3) \quad (31)$$

with the solution

$$P_t \sim \frac{2n}{n-1}t^{-1}. \quad (32)$$

This is a special case of the general theorem [17]

$$P_t \sim \frac{2}{tg''(1)} \quad (33)$$

for a critical branching process.

The next quantity of interest is the size distribution of the earthquakes. With \mathcal{D}_s we denote the probability that the size of an avalanche is exactly s . While $\mathcal{D}_1 = (1-1/n)^n$ is obvious, the calculation of \mathcal{D}_s for $s > 1$ proceeds as in [18]. We first denote by $a_k^{(s)}$ the k -th Taylor coefficient of $[g(u)]^s$, i.e. $[g(u)]^s = a_0^{(s)} + a_1^{(s)}u + a_2^{(s)}u^2 + \dots$. A theorem due to Dwass [22] tells us then that

$$\mathcal{D}_s = \frac{1}{s}a_{s-1}^{(s)}, \quad s \geq 1. \quad (34)$$

In the present case, we have

$$a_k^{(s)} = \binom{ns}{k}(1-p)^{ns-k}p^k, \quad (35)$$

leading to

$$\mathcal{D}_s = \frac{1}{s} \binom{ns}{s-1} (1-p)^{(n-1)s+1} p^{s-1}. \quad (36)$$

The local limit theorem of Moivre–Laplace states that in the limit $s \rightarrow \infty$ the distribution \mathcal{D}_s with $p = 1/n$ tends to

$$\mathcal{D}_s \approx \frac{1}{\sqrt{2\pi(1-1/n)}} s^{-3/2}. \quad (37)$$

This means that the system gets critical for $\alpha = 1/n$, and the critical exponents take the same values as for mean-field percolation [21].

In the subcritical phase the arguments are more tedious. Let us denote by $c_i(z)$ the joint probability distribution that a discharge happens during the i -th generation of an earth quake, and that the discharging site has force z . It is related to $C(z)$ and to p_i by

$$C(z) = \frac{1}{\langle s \rangle} \delta(z-1) + c_1(z) + c_2(z) + \dots \quad (38)$$

and

$$p_i = \frac{\int_1^{1/(1-\alpha)} c_i(z) dz}{n \int_1^{1/(1-\alpha)} c_{i-1}(z) dz}. \quad (39)$$

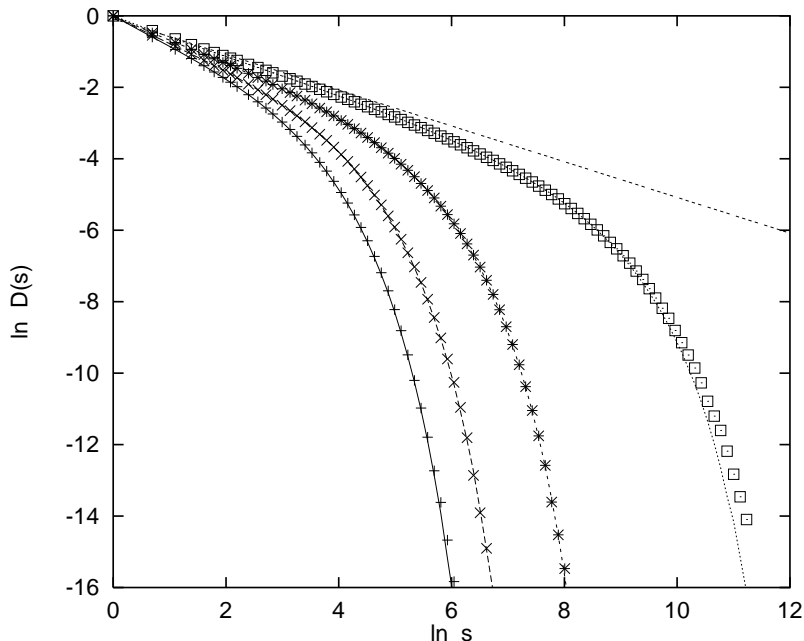


Figure 5: The integrated distribution $D_s = \sum_{s'=s}^{\infty} D_{s'}$ with the same α -values as in fig. 4. The dashed line shows the scaling law $D_s = \frac{2}{\sqrt{2\pi(1-1/n)}} s^{-1/2}$.

This is easily checked by noting that it is compatible with

$$\langle s \rangle = 1 + np_1 + n^2 p_1 p_2 + n^3 p_1 p_2 p_3 + \dots \quad (40)$$

The functions $c_i(z)$ satisfy a recursion relation similar to eq.(16),

$$c_i(z) = n \Theta(z-1) \int_1^{1/(1-\alpha)} P(z - \alpha z') c_{i-1}(z') dz' \quad (41)$$

with $c_0(z) = \delta(z-1)/\langle s \rangle$. Again we were not able to solve this analytically. But given a numerical estimate of $P(z)$ we can solve it numerically for $c_i(z)$, $i = 1, 2, \dots$, from which we obtain p_i by integration. Again this was done only for $n = 4$. For each considered value of α we found that p_i increases monotonically with i and converges very quickly to a constant value $< 1/4$. This is easy to understand. The increase is due to the fact that the first discharging site has $z = 1$, while all subsequent ones have z slightly larger than 1. The fact that $p_i < 1/4$ reflects the fact that we are dealing with a subcritical branching process.

In contrast to the critical case we now have a time dependent (non-autonomous) branching process, i.e. the generating function $g(u)$ depends on the generation. The mathematical treatment becomes now more tedious. For the further comparison between simulations and theory we therefore used the theoretically obtained p_i to simulate a branching process, and compared the results with direct simulations of the OFC model. Figures 4 and 5 show that the agreement is essentially perfect, except for large s and t , and for $\alpha = 0.23$. The discrepancies seen there arise from the numerical problems mentioned in sec.3.

6 The Feder-Feder Model

Up to now we have considered only the OFC model, but our methods are much more general. To illustrate this, we shall discuss in this section the random-neighbor version of a model introduced by Feder and Feder (FF) [23]. The FF model is identical to OFC model, with the only exception that eq.(2) is replaced by

$$z_{j_k} \rightarrow z_{j_k} + \alpha, \quad k = 1, \dots, n. \quad (42)$$

This means that a site hit by a discharge always receives a fixed amount α regardless of the z -value of the discharging site. This leads to a significant simplification of the equations of motion. To derive them, we have first of all to notice that the *toppling rate* is now given by

$$\sigma = \frac{\langle s \rangle}{N(1 - \bar{z}_m)} = \frac{1}{z_{unst} - n\alpha}. \quad (43)$$

Since $z_{unst} \geq 1$, it is not a priori clear whether σ diverges in the limit $\alpha \rightarrow 1/n$. But we will show that this is indeed the case.

The main simplification arises from the fact that $Q_1(\Delta z)$ uncouples from $C(z)$ and is given by

$$Q_1(\Delta z) = \delta(\Delta z - \alpha). \quad (44)$$

From this one obtains immediately

$$Q_k(\Delta z) = \delta(\Delta z - k\alpha), \quad (45)$$

see eq.(14), and

$$P(z) = \sum_{j=0}^m P_j(z) = \sum_{j=0}^m \frac{\sigma}{j!} (n\sigma(z - j\alpha))^j \Theta(z - j\alpha) e^{-n\sigma(z - j\alpha)}, \quad (46)$$

where m is again the largest integer $\leq 1/\alpha$. To obtain σ as a function of α , we use the normalization condition $\int_0^1 P(z) dz = 1$ which gives

$$n = \sum_{j=0}^m \frac{1}{j!} \int_0^{(1-\alpha j)n\sigma} dx x^j e^{-x}. \quad (47)$$

For α close to $1/n$ we have $m = n$, and this condition can be rewritten as

$$\int_0^{\epsilon n\sigma} dx x^n e^{-x} = \sum_{j=0}^{n-1} \frac{n!}{j!} \int_{(1-\alpha j)n\sigma}^{\infty} dx x^j e^{-x}, \quad (48)$$

where we have used again $\epsilon = 1 - n\alpha$. From this it is easily seen that $\sigma \rightarrow \infty$ for $\epsilon \rightarrow 0$. Otherwise, the left hand side would tend to zero in this limit, while the r.h.s. would remain non-zero. But if σ diverges, the r.h.s. is dominated by the term with $j = n - 1$. Keeping only dominant terms we arrive at

$$\sigma \approx (n + 1) \log(1/\epsilon). \quad (49)$$

The mean avalanche size can again be calculated from eq.(5),

$$\langle s \rangle = \sigma/P(1) = \left[\sum_{j=0}^m \pi_j (1 - j\alpha) \right]^{-1}. \quad (50)$$

Obviously $\langle s \rangle$ is finite for all $\alpha < 1/n$ and diverges for $\alpha \rightarrow 1/n$. In this limit the sum is dominated by the term with $j = n$, giving

$$\langle s \rangle \approx n! (n\sigma\epsilon)^{-n} \sim \epsilon^{-n}, \quad (51)$$

up to constant and logarithmic factors in ϵ which could easily be computed.

Thus σ and $\langle s \rangle$ both diverge much slower than in the OFC model. This reflects the increased dissipation in the FF model. Exact values of σ and $\langle s \rangle$ obtained numerically from eqs.(47) and (50) are shown in fig.6. For small ϵ one finds good agreement with the asymptotic predictions. Avalanche dynamics can be treated exactly as in the OFC model.

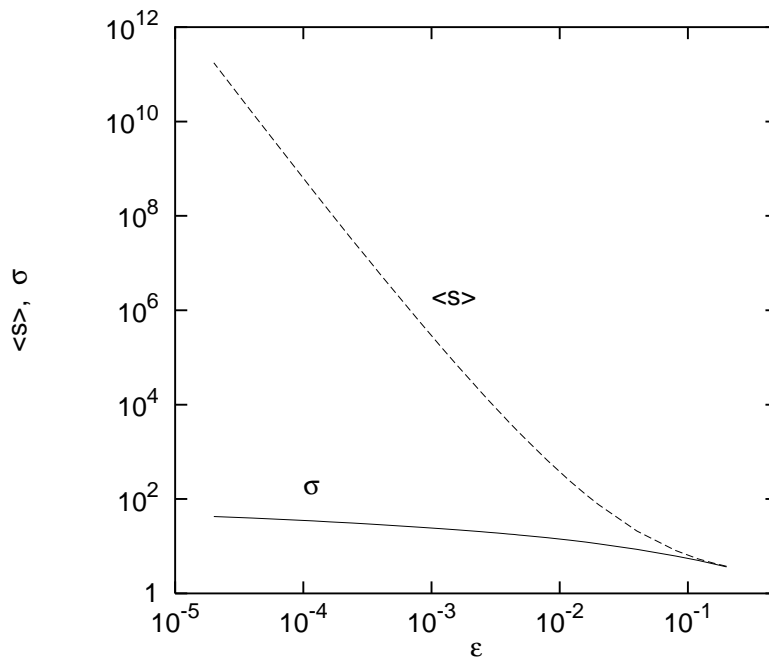


Figure 6: Log-log plot of σ and $\langle s \rangle$ against $\epsilon = 1 - 4\alpha$ for the Feder-Feder model.

7 Conclusion

Our results show clearly that there are neither scaling nor phase transitions in the random neighbor version of the dissipative Olami-Feder-Christensen earthquake model. Scaling is observed only in the conservative limit, in which case one has a critical branching process. This is in direct contradiction to claims in [12]. The latter was

based on approximate random neighbor equations, while the present work is based on the exact equations. These equations were solved numerically, giving excellent agreement with direct simulations of the model.

The most surprising result was the very fast increase of the average earth quake size as one approaches the conservative limit. Obviously this is a consequence of the non-locality of the interaction, since this implies that one can have extremely large earth quakes without having large effects locally. Nevertheless, avalanche size distributions decay exponentially for any non-zero dissipation.

Our findings support the view [6] that scaling in the OFC model with inhomogeneous boundary conditions is due to a subtle interplay between partial synchronization and desynchronization. The inhomogeneity of the bc drives the synchronization in the bulk, building up large coherent patches, but occasionally the driving is too strong and the synchronization breaks down. Explicit observations of these patterns [6, 8] support this view. In a random neighbor model such structures cannot build up, of course, and the mechanism driving the system into a self-organized critical state is absent.

While we concentrated here on the OFC model, we showed that our methods can also be applied in other related models. In particular, we studied the Feder-Feder model in some detail. We showed that it also has no phase transition in the dissipative regime, and that the toppling rate and the mean avalanche size diverge in the conservative limit.

Acknowledgement:

The authors want to thank H. Flyvberg for interesting discussions. This work was supported by the DFG within the Graduiertenkolleg ‘Feldtheoretische und numerische Methoden in der Elementarteilchen- und Statistischen Physik’, and within Sonderforschungsbereich 237.

References

- [1] P. Bak, C. Tang, and K. Wiesenfeld, Phys. Rev. Lett. **59** 381 (1987)
- [2] Z. Olami, H.J.S. Feder, and K. Christensen, Phys. Rev. Lett. **68** 1244 (1992)
- [3] K. Christensen and Z. Olami, Phys. Rev. **A 46**, 1829 (1992)
- [4] R. Burridge and L. Knopoff, Bull. Seismol. Soc. Am. **57** 341 (1967)
- [5] S.S. Manna, L.B. Kiss, and J. Kertesz, J. Stat. Phys. **61** 923 (1990)
- [6] P. Grassberger, Phys. Rev. **E 49**, 2436 (1994)
- [7] A. Corral, C.J. Perez, A. Diaz-Guilera, and A. Arenas, Phys. Rev. Lett. **74**, 118 (1995)
- [8] A.A. Middleton, and C. Tang, Phys. Rev. Lett. **74**, 742 (1995)
- [9] J.E.S. Socolar, G. Grinstein, and C. Jayaprakash, Phys. Rev. **E 49**, 2366 (1993)
- [10] I.M. Jánosi and J. Kertesz, Physica **A 200**, 179 (1993)
- [11] F. Torvund and J. Froyland, Physica Scripta **52**, 624 (1995)
- [12] S. Lise and H.J. Jensen, Phys. Rev. Lett. **76**, 2326 (1996)
- [13] D. Dhar, Phys. Rev. Lett. **64**, 1613 (1990)
- [14] Y.-C. Zhang, Phys. Rev. Lett. **63**, 470 (1989)
- [15] H. Flyvbjerg, Phys. Rev. Lett. **76**, 940 (1996)
- [16] R. Bundschuh and M. Lässig, Phys. Rev. Lett. **77**, 4273 (1996)
- [17] T.E. Harris, *The Theory of Branching Processes* (Springer, Berlin 1969)
- [18] H.-M. Bröker and P. Grassberger, Europhys. Lett., **30** 319 (1995)
- [19] P. Grassberger, J. Phys. **A 26**, 1023 (1992)
- [20] P. Grassberger and S.S. Manna, J. Physique (Paris) **51**, 1077 (1990)
- [21] D. Stauffer, *Introduction to Percolation Theory* (Taylor & Francis, London 1985)
- [22] M. Dwass, J. Appl. Prob. **6**, 682 (1969)
- [23] H. Feder and J. Feder, Phys. Rev. Lett. **66**, 2669 (1991)